

Comparative Studies on Interactions of Bovine Serum Albumin with Cationic Gemini and Single-Chain Surfactants

Yajuan Li, Xiaoyong Wang, and Yilin Wang*

Key Laboratory of Colloid and Interface Science, Institute of Chemistry, Chinese Academy of Sciences, Beijing 100080, People's Republic of China

Received: January 25, 2006; In Final Form: March 6, 2006

The interactions of bovine serum albumin (BSA) with cationic gemini surfactants alkanediyl- α,ω -bis-(dodecyldimethylammonium bromide) $[\text{C}_{12}\text{H}_{25}(\text{CH}_3)_2\text{N}(\text{CH}_2)_S\text{N}(\text{CH}_3)_2\text{C}_{12}\text{H}_{25}]\text{Br}_2$ (designated as $\text{C}_{12}\text{C}_S\text{C}_{12}\text{Br}_2$, $S = 3, 6$, and 12) and single-chain surfactant dodecyltrimethylammonium bromide (DTAB) have been studied with isothermal titration microcalorimetry, turbidity, fluorescence spectroscopy, and circular dichroism at pH 7.0. Comparing with DTAB, $\text{C}_{12}\text{C}_S\text{C}_{12}\text{Br}_2$ have much stronger binding ability with BSA to induce the denaturation of BSA at very low molar ratio of $\text{C}_{12}\text{C}_S\text{C}_{12}\text{Br}_2/\text{BSA}$, and $\text{C}_{12}\text{C}_S\text{C}_{12}\text{Br}_2$ have a much stronger tendency to form insoluble complexes with BSA. The binding of $\text{C}_{12}\text{C}_S\text{C}_{12}\text{Br}_2$ to BSA generates larger endothermic peaks. The first endothermic peak is much stronger than that of the second endothermic peak. The double charges and strong hydrophobicity of the gemini surfactants are the main reasons for these observations. In addition, the spectra results show that the binding of DTAB to BSA only promotes BSA unfolding and aggregation, whereas the secondary structure of BSA is possibly stabilized by a small amount of $\text{C}_{12}\text{C}_S\text{C}_{12}\text{Br}_2$, even if the small amount of binding $\text{C}_{12}\text{C}_S\text{C}_{12}\text{Br}_2$ could induce the loss of the tertiary structure of BSA. This result may be related to the double tails of gemini surfactants, which may generate the hydrophobic linkages between the nonpolar residues of BSA.

Introduction

Protein–surfactant interactions have been a subject of extensive studies over the past few decades because they are of importance in a wide variety of industrial, biological, pharmaceutical, and cosmetic systems.^{1–3} Studies on the interactions of surfactants with proteins can contribute toward an understanding of the action of surfactants as denaturants and as solubilizing agents for proteins. Extensive studies on the interactions of surfactants with proteins have been reported and reviewed.^{4–6}

Usually, surfactants binding with proteins depend on surfactant features. Anionic surfactants interact strongly with proteins and cause their denaturation.^{7–11} The denaturation is possible due to the unfolding of proteins induced by surfactants. Comparing with anionic surfactants, cationic surfactants exhibit a lower tendency to interact with proteins mainly as a consequence of a smaller relevance of electrostatic interaction at the pHs of interest.¹² However, the shapes of binding isotherms of these two kinds of surfactants with the same protein are similar.^{12,13} The binding isotherms of protein with surfactant show four characteristic regions with an increase in surfactant concentration.¹⁴ The initial region, at very low surfactant concentration, is associated with the binding of surfactant monomers to the specific high-energy sites of the proteins and the interactions are electrostatic in nature. The second region corresponds to a slowly rising part or an apparent plateau. The bound surfactants may not affect the binding of other surfactants to BSA due to the long distance of binding sites. That is, the binding in this region is noncooperative. The third region corresponds to a massive increase in binding caused by

cooperative interactions of surfactants with already bound surfactant molecules. The unfolding of proteins is believed to start in this region. For the fourth region, beyond the saturation point, the binding isotherm shows a plateau, suggesting that the excess surfactant molecules will not bind to protein any more and normal micelles start to form.

In recent years, cationic gemini surfactants have been well developed. These surfactants are made up of two hydrophobic chains and two polar headgroups covalently linked through a spacer group.^{15–18} These kinds of surfactants have a number of unique aggregation properties in comparison to conventional single-chain surfactants, such as much lower critical micelle concentration (cmc), strong dependence on spacer structure, special aggregate morphology, strong hydrophobic microdomain, and so on. Thus, gemini surfactants are expected to exhibit quite different interaction behavior with protein from single-chain surfactants.

In the present work, we focus on the interaction of cationic gemini surfactants with bovine serum albumin (BSA) using microcalorimetry, turbidity, steady-state fluorescence, and circular dichroism. BSA is a globular protein. In its native state, it has a molar mass of 66.4 kDa and possesses about 583 amino acids¹⁹ with 17 disulfide bonds and one free cysteine group.²⁰ It has relatively high water solubility because of its large number of ionizable amino acids.²¹ BSA can bind many different types of amphiphilic biological molecules, which are believed to play an important role in determining the physiological function.²² The cationic gemini surfactants alkanediyl- α,ω -bis(dodecyldimethylammonium bromide) have the structure of $[\text{C}_{12}\text{H}_{25}(\text{CH}_3)_2\text{N}(\text{CH}_2)_S\text{N}(\text{CH}_3)_2\text{C}_{12}\text{H}_{25}]\text{Br}_2$, designated as $\text{C}_{12}\text{C}_S\text{C}_{12}\text{Br}_2$, where $S = 3, 6$, and 12 , indicating the number of carbons in the spacer. For comparison, parallel measurements have also been made

* To whom the correspondence should be addressed. E-mail: yilinwang@iccas.ac.cn.

on the interaction between single-chain surfactant dodecyltrimethylammonium bromide (DTAB) and BSA.

Experimental Section

Materials. Gemini surfactants $C_{12}C_3C_{12}Br_2$ ($S = 3, 6$, and 12) were synthesized and purified according to the method of Menger and Littau.¹⁷ Dodecyltrimethylammonium bromide (DTAB, purity >99%) from Aldrich was recrystallized twice before use. Bovine serum albumin (BSA) was purchased from Sigma and dialyzed and lyophilized before use. All samples were prepared in 5 mM sodium phosphate buffer of ionic strength 0.01 mol/L at pH 7.0. The BSA concentration was determined by UV-absorbance measurement (Shimadzu 1601PC UV/vis spectrophotometer), using a molar extinction coefficient of $4.4 \times 10^4 \text{ M}^{-1} \text{ cm}^{-1}$ at 280 nm.²³ The BSA concentration was kept at 1 g/L (0.015 mM) in all measurements. All other reagents used were of analytical grade and water was triply distilled.

Isothermal Titration Microcalorimetry (ITC). The calorimetric measurements were conducted with a TAM 2277-201 microcalorimetric system (Thermometric AB, Järfälla, Sweden) with a stainless steel sample cell of 1 mL at $298.15 \pm 0.01 \text{ K}$. The cell was initially loaded with 0.7 mL of pH 7.0 buffer or 1 g/L BSA in pH 7.0 buffer. The concentrated surfactant solutions were injected into the sample cell via a 250- μL Hamilton syringe controlled by a 612 Thermometric Lund pump. The system was stirred at 50 rpm with a gold propeller. All experiments were repeated twice, and the reproducibility was within $\pm 2\%$. The accuracy of the calorimeter was periodically calibrated electrically and verified by measuring the dilution enthalpies of concentrated sucrose solution.²⁴ The observed enthalpy (ΔH_{obs}) was obtained by integration over the peak for each injection in the plot of heat flow P against time t .

Turbidity Measurements. Turbidity measurements were carried out with a Shimadzu 1601 PC UV/vis spectrometer. The turbidity of the surfactant/BSA mixed solutions was monitored by UV absorbance at 360 nm. A cuvette with 1 cm pathway was used. All the measurements were conducted at $298.15 \pm 0.5 \text{ K}$.

Fluorescence Measurements. The fluorescence intensities were measured with a Hitachi F-4500 spectrofluorometer. The excitation wavelength was 295 nm, and the emission spectra were scanned from 305 to 450 nm. A quartz cell with 1 cm path length was used. All the measurements were conducted at $298.15 \pm 0.5 \text{ K}$.

Circular Dichroism Measurements (CD). CD spectra were recorded on a JASCO J-810 spectrophotometer, using a bandwidth of 1.0 nm, a step interval of 0.5 nm, and an integration time of 0.5 s. Far-UV CD spectra were acquired with use of a cell of 0.1 mm path length over the wavelength range between 200 and 250 nm. Four scans were averaged and smoothed to improve signal-to-noise ratio. The results were expressed in terms of mean residue molar ellipticity $[\theta]$, in units of $\text{deg} \cdot \text{cm}^2 \cdot \text{dmol}^{-1}$, taking a value of 113 as the mean residue weight for BSA.²⁵ All the measurements were conducted at $298.15 \pm 0.5 \text{ K}$.

Results

The micellization of three gemini surfactants $C_{12}C_3C_{12}Br_2$ ($S = 3, 6$, and 12) and DTAB in 5 mM pH 7.0 phosphate buffer was first studied by isothermal titration microcalorimetry. The calorimetric titration curves of the observed enthalpy (ΔH_{obs}) with the final surfactant concentration (C) are presented in Figure 1. All the titration curves have an approximately

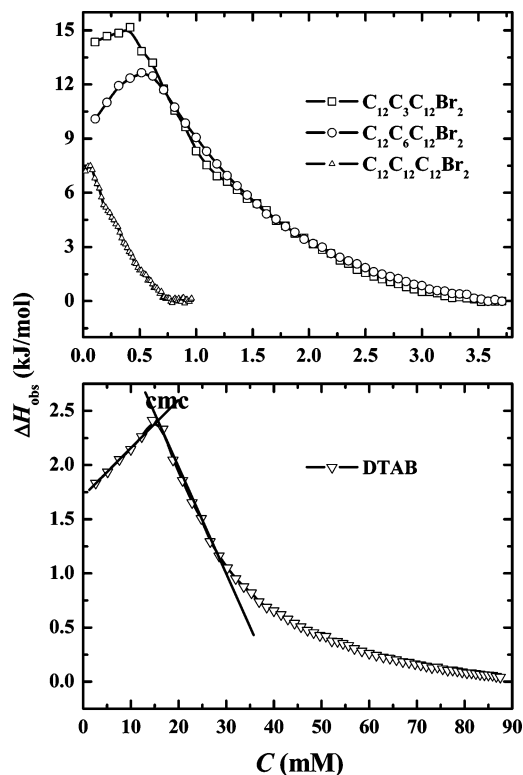


Figure 1. Calorimetric titration curves for $C_{12}C_3C_{12}Br_2$ and DTAB into pH 7.0 phosphate buffer against the final surfactant concentration at 298.15 K.

TABLE 1: Critical Micelle Concentration for $C_{12}C_3C_{12}Br_2$ and DTAB in 5 mM pH 7.0 Phosphate Buffer at 298.15 K

	surfactants			
	DTAB	$C_{12}C_3C_{12}Br_2$	$C_{12}C_6C_{12}Br_2$	$C_{12}C_{12}C_{12}Br_2$
cmc (mM)	14.53 ± 0.29	0.40 ± 0.01	0.56 ± 0.03	0.07 ± 0.01
cmc ^a (mM)	15.47	0.85	0.89	0.29

^a cmc value in water from refs 28 and 29.

sigmoidal shape with an abrupt decrease at a threshold concentration corresponding to the micelle formation, allowing identification of the critical micelle concentration (cmc) by an extrapolation of the initial portion of the curve and of the rapidly decreasing portion of the curve,^{26,27} as shown in Figure 1b. When C is below cmc, the enthalpy change results from the dilution of micelles, the breakup of the added micelles, and the further dilution of the monomers. When C is above cmc, only the added micelles are diluted and finally ΔH_{obs} drops toward zero. The obtained cmc values are presented in Table 1. For comparison, the cmc values in water^{28,29} are also presented. As shown, the cmc values of all the studied surfactants in buffer are lower than those in water. It is worthy to note that the decrease of cmc for gemini surfactants is more marked in comparison with the slight decrease of cmc for DTAB. In buffer, micelle formation can be promoted by added salt because of the screening of the electrostatic repulsion among surfactant headgroups. For $C_{12}C_3C_{12}Br_2$, due to the two headgroups, the electrostatic repulsion may reduce to a more significant extent. The micellization would be much more significantly promoted, leading to the distinctly decreased cmc. Meanwhile, the cmc values of gemini surfactants are much lower than that of DTAB. This observed phenomenon has been found by other authors.^{30,31} There are two alkyl chains for gemini surfactants transferred from aqueous to the micelle core during the micellization process, which results in the stronger hydrophobic interaction

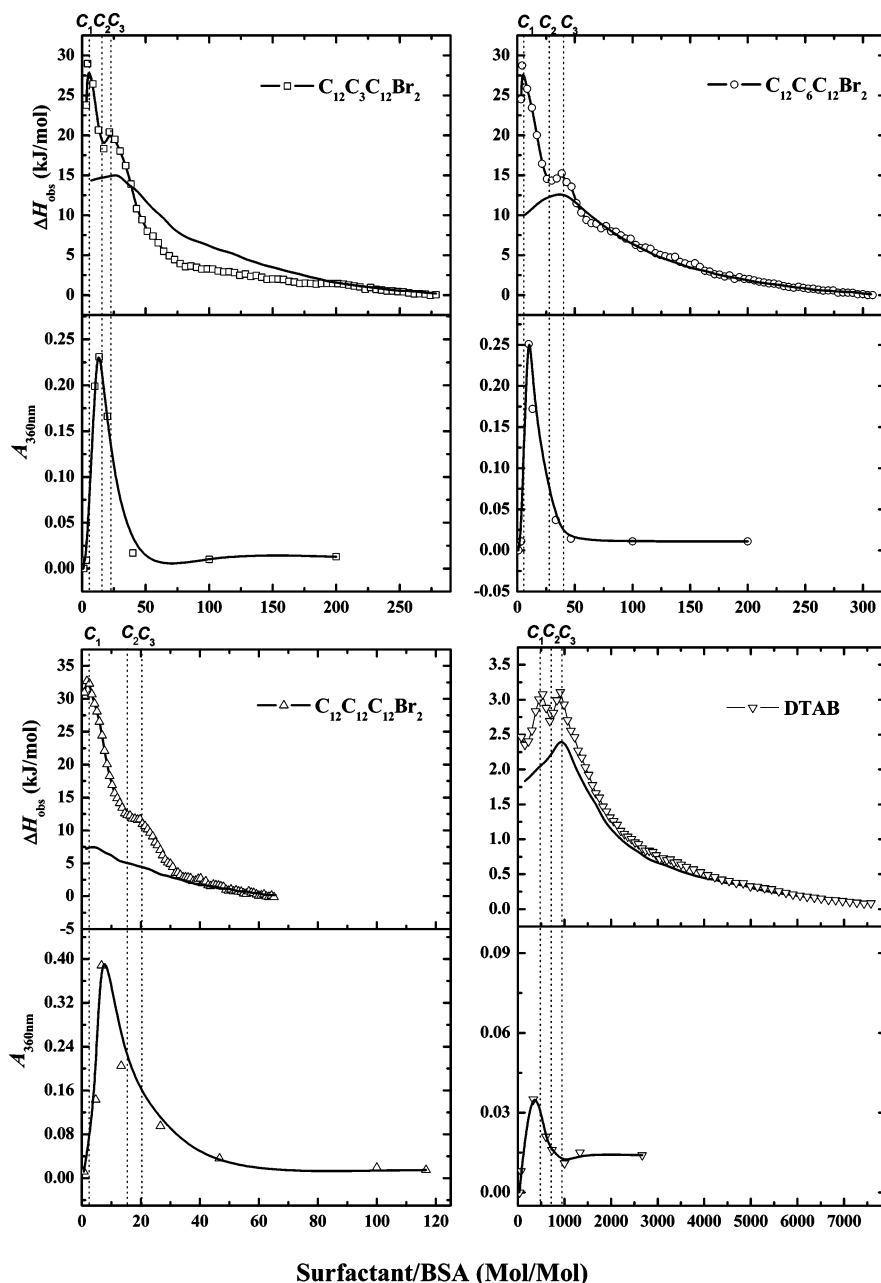


Figure 2. Calorimetric titration curves and turbidity curves for $C_{12}C_5C_{12}Br_2$ and DTAB into 1 g/L BSA in pH 7.0 phosphate buffer against the molar ratio of surfactant to BSA at 298.15 K. Solid lines correspond to the curves for the surfactants into buffer against the corresponding surfactant concentration without BSA.

among the gemini surfactant chains. In addition, for these three gemini surfactants, the cmc value of $C_{12}C_{12}C_{12}Br_2$ is much lower than those for $C_{12}C_3C_{12}Br_2$ and $C_{12}C_6C_{12}Br_2$. The reason is that the longer spacer of $C_{12}C_{12}C_{12}Br_2$ may adopt a looped conformation within the hydrophobic core, leading $C_{12}C_{12}C_{12}Br_2$ molecules to have stronger hydrophobic interaction with each other.³²

To study the interaction of $C_{12}C_5C_{12}Br_2$ and DTAB with BSA, ITC and turbidity measurements by UV were conducted to monitor the enthalpy change and the complex formation in the studied systems. Figure 2 shows the variation of ΔH_{obs} for $C_{12}C_5C_{12}Br_2$ and DTAB titrated into 1 g/L of BSA solution and turbidimetric curves of the surfactant/BSA mixed solutions with the molar ratio of surfactants to BSA at pH 7.0.

The calorimetric titration curves in BSA solution become pronouncedly different from the characteristic sigmoidal shape seen for the surfactants in the absence of BSA. The differences

can be attributed to the interactions between BSA and the surfactants. These calorimetric curves for the different surfactants show the same basic features and have similar shapes, characterized by two endothermic peaks. Moreover, both of the peaks for $C_{12}C_5C_{12}Br_2$ with BSA are much more positive than those for DTAB with BSA. With the first several injections of the surfactants into BSA solution, ΔH_{obs} increases until the maximum point C_1 of the first peak. Then, with the further addition of the surfactants, ΔH_{obs} decreases until point C_2 . Beyond point C_2 , ΔH_{obs} rises again until the maximum point C_3 of the second peak. After point C_3 , ΔH_{obs} decreases again and then the curve coincides with the dilution curve of the corresponding surfactants in the absence of BSA. Corresponding to the above enthalpy variations, the mixed solution is transparent and the turbidity is close to zero at a low molar ratio of surfactant to BSA. With increasing the ratio of surfactant to BSA, the turbidity increases rapidly up to a maximum value.

Accordingly, the mixed solution becomes opaque. Beyond the maximum value, the turbidity decreases, and finally the turbidity becomes small and constant again. As a result, the mixed solution becomes transparent again. Because the abrupt changes of turbidity arise mainly from the change of the amount and size of aggregates in the solution, the above changes of turbidity are supposed to occur due to the formation and the redissolution of the surfactant/BSA complexes.^{33–35} Furthermore, the larger increasing in solution turbidity between C_1 and C_2 for $C_{12}C_3C_{12}Br_2$ is an indication of the formation of aggregates that are large enough to induce phase separation. Interestingly, it is noted that both the first peak in the calorimetric curves and the maximum turbidity values for the gemini surfactants with BSA are much larger than those for DTAB with BSA, and the corresponding ratios for the gemini surfactants to BSA being much lower than those for DTAB to BSA, even a very small amount of the gemini surfactants have caused the systems to exhibit significant change. These complicated enthalpy curves as well as the turbidity variations must be accompanied by the structural variation of BSA and the variation of the binding behavior of BSA with the surfactants.

To aid the interpretation of ITC and turbidity data, the fluorescence and circular dichroism experiments were used to study the structural variation. As indicated by the turbidity, there are soluble surfactant/BSA complexes with the initial binding of surfactants, and all surfactant/BSA complexes are dissociated again after the addition of more surfactants. So, we performed the fluorescence and CD experiments on native BSA and BSA mixed with the studied surfactants at different surfactant/BSA ratios. The molar ratios of surfactant to BSA used are 65, 1, 1, and 1 for DTAB, $C_{12}C_3C_{12}Br_2$, $C_{12}C_6C_{12}Br_2$, and $C_{12}C_{12}C_{12}Br_2$, respectively, which correspond to the region of the surfactant/BSA ratio before C_1 , where obvious binding with BSA has occurred and the soluble complexes are formed. And the molar ratios of surfactant to BSA are 1000, 100, 100, and 46 for DTAB, $C_{12}C_3C_{12}Br_2$, $C_{12}C_6C_{12}Br_2$, and $C_{12}C_{12}C_{12}Br_2$, respectively, which correspond to the region of the surfactant/BSA ratio beyond C_3 , where all of the insoluble complexes are dissociated into soluble complexes again. Between C_1 and C_3 , the fluorescence and CD experiments could not be conducted precisely due to the existence of insoluble complexes.

BSA is constituted by around 583 amino acid residues, whereas its secondary structure contains 67% α -helix structure and 17 disulfide bridges that confer relatively strong stability on BSA.^{36,37} Its tertiary structure is composed of three domains. Each domain includes about 190 amino acid residues with a molecular weight of approximately 22 000.³⁸ Fluorescence excited at 295 nm was used to monitor the changes on the tertiary structure of BSA induced by the interaction with $C_{12}C_3C_{12}Br_2$ and DTAB. These interactions can, in principle, produce changes in the position or orientation of the tryptophan residues, altering their exposure to solvent.³⁹ Figure 3 illustrates the emission spectra of native BSA and BSA mixed with DTAB and $C_{12}C_3C_{12}Br_2$. It is observed that the intrinsic fluorescence intensities decrease when the molar ratios of surfactant to BSA are before C_1 for DTAB, $C_{12}C_3C_{12}Br_2$, $C_{12}C_6C_{12}Br_2$, and $C_{12}C_{12}C_{12}Br_2$, respectively. Furthermore, the intrinsic fluorescence intensities decrease further as the ratios increase beyond C_3 . At the same time, the decrease of the intrinsic fluorescence intensity is accompanied by a slight blue shift in the maximum of emission wavelength. These kinds of changes for DTAB are somewhat stronger than those for $C_{12}C_3C_{12}Br_2$ due to the relatively higher ratio of DTAB to BSA. For $C_{12}C_3C_{12}Br_2$, the

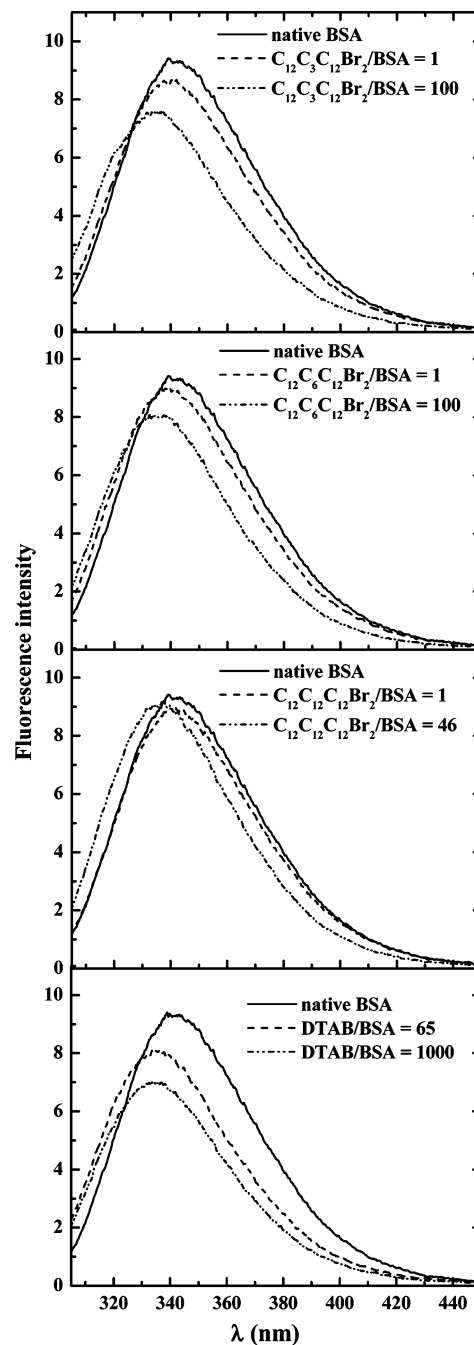


Figure 3. Fluorescence spectra of 1 g/L native BSA (solid line) and of BSA treated with surfactants. The dash line and dash-dot-dot line correspond to the molar ratios before C_1 or beyond C_3 , respectively.

decreasing extent of fluorescence intensity is slightly weaker for the gemini surfactant with a longer spacer length.

Circular dichroism measurements were performed to monitor the changes of the secondary structure generated by the interaction of BSA with $C_{12}C_3C_{12}Br_2$ and DTAB. Typical far-UV CD spectra for native BSA and for BSA in the presence of the studied surfactants are shown in Figure 4. It is observed that when DTAB is added to BSA, the magnitude of molar ellipticity decreases. However, as the ratios of surfactant to BSA are before C_1 for $C_{12}C_3C_{12}Br_2$, $C_{12}C_6C_{12}Br_2$, and $C_{12}C_{12}C_{12}Br_2$, respectively, the magnitude of molar ellipticity shows little change for $C_{12}C_3C_{12}Br_2$ and a somewhat increase for $C_{12}C_6C_{12}Br_2$ and $C_{12}C_{12}C_{12}Br_2$. When the ratios are increased beyond C_3 for $C_{12}C_3C_{12}Br_2$, $C_{12}C_6C_{12}Br_2$, and $C_{12}C_{12}C_{12}Br_2$, respectively, the molar ellipticity decreases distinctly.

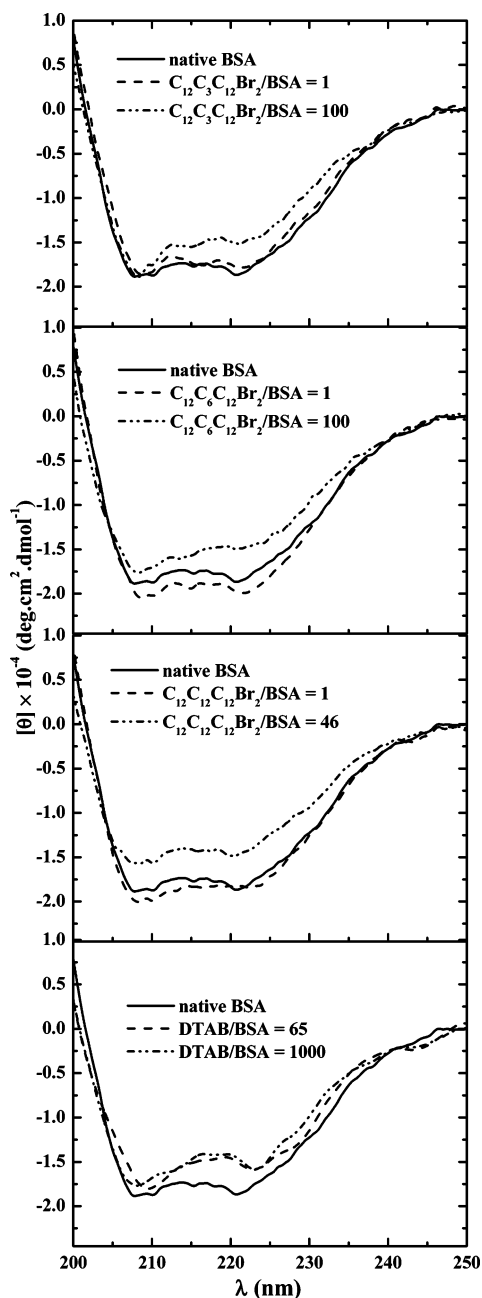


Figure 4. Circular dichroism (CD) spectra of 1 g/L native BSA (solid line) and of BSA treated with surfactants. The dash line and dash-dot-dot line correspond to the molar ratios before C_1 or beyond C_3 , respectively.

Discussion

Combining the results from microcalorimetry, turbidity, and spectra measurements, the binding mechanism for $C_{12}C_5C_{12}Br_2$ and DTAB to BSA is proposed in Figure 5.

When the molar ratio of surfactant to BSA is lower than C_1 , some surfactant monomers electrostatically bind on BSA, where the binding of DTAB causes the instability of BSA; however, binding of $C_{12}C_5C_{12}Br_2$ to BSA would stabilize the secondary structure of BSA although the environment of tryptophan is transferred into one of a less polarity. The binding of monomers to BSA forms the complex as indicated by an increase in turbidity and the increasing of ΔH_{obs} in the calorimetric curve. Meanwhile, at a very low ratio of surfactant to BSA, although there may be some positive charged surfactant monomers binding to negatively charged groups of BSA and then reducing

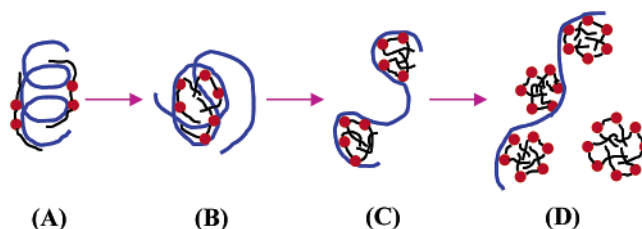


Figure 5. Schematic representation of the interaction of BSA with the surfactants: (A) surfactant/BSA < C_1 , (B) C_1 < surfactant/BSA < C_2 , (C) C_2 < surfactant/BSA < C_3 , and (D) surfactant/BSA > C_3 .

the net negative charges of BSA, the negative charges of BSA are still large enough to make the surfactant/BSA complexes soluble. As the surfactant/BSA ratio increases, the insoluble surfactant/BSA complexes are formed. $C_{12}C_5C_{12}Br_2$ have double tails, which may act as the hydrophobic linkages between the nonpolar residues on BSA. The protein structure may be protected by such linkages.⁴⁰ The secondary structure α -helix of BSA is, therefore, stabilized, indicated by the slightly increased molar ellipticity. In contrast, DTAB may not produce this kind of hydrophobic linkages due to the single tail. As a result, the binding of DTAB to BSA leads to the instability of the BSA secondary structure, reflected in the decreased molar ellipticity. In general, for proteins with tryptophan, both changes in fluorescence intensity and shifts in wavelength indicate the unfolding of protein.⁴¹ As is well-known,⁴¹ tryptophan emission occurs at shorter wavelength in a hydrophobic environment. Thus, the maximum of emission wavelength shifting toward shorter wavelength means that BSA may have transferred to a more hydrophobic environment composed of the bound surfactants. Meanwhile, the exposure of tryptophan residues to a more hydrophobic environment leads to a decrease in the intrinsic fluorescence intensity.

When the molar ratio of surfactant to BSA is between C_1 and C_2 , the surfactants bind to BSA molecules cooperatively, which promotes the partial unfolding and the aggregation of the surfactant/BSA complexes. The micelle-like aggregates may be formed due to the hydrophobic interaction between the surfactants with already bound surfactant molecules. The evidence for this assertion is the decreasing of ΔH_{obs} and the increasing turbidity. Besides, as BSA binds more surfactant molecules, the net electrical charges on the complexes would tend toward zero, resulting in the maximum value of turbidity. Beyond a certain surfactant concentration, the net positive charges on the complexes owing to the binding by more cationic surfactant molecules would be sufficiently large enough to oppose aggregation and lead to a redissolution of the complexes, corresponding to a decrease in turbidity. Furthermore, the excess binding of surfactants may lead to unfavorable electrostatic repulsion among the bound surfactants and destabilize the BSA structure.

When the molar ratio of surfactant to BSA is between C_2 and C_3 , BSA is denatured and the surfactants will bind to the unfolded BSA to form micelle-like aggregates. Here, owing to a larger amount of bound surfactant molecules, the aggregates are different from the aggregates between C_1 and C_2 . After the unfolding of BSA, there would be an increase in the number of exposed nonpolar groups, to which many more surfactant molecules could bind through hydrophobic interaction. The formation of micelle-like aggregates should be an exothermic process, opposite of demicellization. Thus, the increasing of positive ΔH_{obs} may therefore indicate that BSA denaturation superimposes upon the surfactant binding. In addition, the electrostatic repulsion among more and more bound micelles

results in an extended BSA structure, and in turn the intrachain hydrophobic bond of BSA may be broken. Therefore, the BSA molecules are greatly denatured with binding of a large amount of the ionic surfactants.

When the molar ratio of surfactant to BSA is beyond C_3 , the free micelles begin to form after the saturation of BSA. The evidence for the formation of free micelle is that there is an appreciable decrease in ΔH_{obs} , which is consistent with that observed in the absence of BSA. Additionally, the decreasing of fluorescence intensity and molar ellipticity may suggest that BSA exists in an exposed structure in the presence of excess surfactants.

On the basis of the above discussion, we could further understand the difference of the binding between single-chain and gemini surfactants to BSA. As shown in Figure 2, the binding of $C_{12}C_5C_{12}Br_2$ to BSA leads to more endothermic ΔH_{obs} than that of DTAB. Meanwhile, the $C_{12}C_5C_{12}Br_2$ /BSA ratio for the first peak in the calorimetric curves is much lower than that for DTAB. Additionally, the endothermic extent of the two peaks for binding DTAB to BSA is comparable with each other. However, for binding $C_{12}C_5C_{12}Br_2$ to BSA, the first peak is much more endothermic than the second peak. Moreover, the maximum values of turbidity for binding $C_{12}C_5C_{12}Br_2$ to BSA are much larger than that of DTAB. As already discussed above, the first endothermic peak in the calorimetric curves is probably related to the binding of surfactant molecules to BSA. Both electrostatic and hydrophobic interactions will occur as the positively charged headgroups of the surfactants bind to negatively charged amino acid residues, while the surfactant hydrophobic chains interact with adjacent hydrophobic regions of BSA. However, the second peak mainly originates from the largely unfolding BSA, which may mainly depend on the hydrophobic interaction. Consequently, different from DTAB, for the binding of $C_{12}C_5C_{12}Br_2$ with BSA, the magnitude of the two peaks becomes more endothermic due to the double charges and double hydrophobic chains, and the increased extent of the first peak is much larger than that of the second peak. On the basis of the same reasoning, $C_{12}C_5C_{12}Br_2$ and BSA may form complexes with large size or in large amount at a very low surfactant/BSA molar ratio, leading to the larger maximum values of turbidity.

The effect of the spacer length on the interaction can also be seen from the above experimental results. From the calorimetric results, the $C_{12}C_5C_{12}Br_2$ /BSA ratios corresponding to the two endothermic peaks are much lower than those for $C_{12}C_3C_{12}Br_2$ and $C_{12}C_6C_{12}Br_2$. Meanwhile, upon increasing the spacer length, the maximum values of turbidity increase. The hydrophobicity of the gemini surfactants increases as the spacer length increases, because the longer spacer facilitates the hydrophobic interaction among the hydrophobic tails. The stronger hydrophobicity of $C_{12}C_5C_{12}Br_2$ may promote the binding of the surfactant molecules to BSA to a more marked degree, resulting in lower molar ratios for the two calorimetric peaks. Additionally, the stronger hydrophobicity has the stronger ability to promote the aggregation of the complexes, resulting in the larger maximum values of turbidity.

Conclusions

The comparative studies on the interactions of bovine serum albumin (BSA) with cationic gemini surfactants $C_{12}C_5C_{12}Br_2$ ($S = 3, 6$, and 12) and single-chain surfactant DTAB have been carried out. Addition of $C_{12}C_5C_{12}Br_2$ into BSA will generate larger endothermic peaks at lower $C_{12}C_5C_{12}Br_2$ /BSA molar

ratios and induce the aggregation to a great extent, indicating the stronger binding ability of $C_{12}C_5C_{12}Br_2$ with BSA. Furthermore, the combination of strong electrostatic and hydrophobic interactions leads to the much more endothermic first peak. Meanwhile, the mechanism for $C_{12}C_5C_{12}Br_2$ binding to BSA is found to be somewhat different from that of DTAB. The binding of DTAB to BSA only results in the unfolding of BSA. However, the binding of $C_{12}C_5C_{12}Br_2$ to BSA plays two opposite roles in the unfolding and the stability of the BSA structure. At low $C_{12}C_5C_{12}Br_2$ /BSA ratio, it can stabilize the secondary structure of BSA although the tertiary structure of BSA is lost. This result may be attributed to the two hydrophobic chains of gemini surfactants, which make the hydrophobic linkages available between the nonpolar residues of BSA. At high $C_{12}C_5C_{12}Br_2$ /BSA ratio, the binding of $C_{12}C_5C_{12}Br_2$ leads to the unfolding of BSA, similar to that of DTAB. The binding of a large number of surfactants may break the intrachain hydrophobic bond of BSA, resulting in an extended structure of BSA.

Acknowledgment. We are grateful for financial support from the National Natural Science Foundation of China (Grant Nos. 20233010 and 20573123).

References and Notes

- (1) McClements, D. J. In *Food Emulsions: Principles, Practice and Techniques*, 2nd ed.; CRC Press: Boca Raton, FL, 2004.
- (2) Jones, M. N. *Chem. Soc. Rev.* **1992**, *21*, 127–136.
- (3) Jones, M. N. In *Food Polymers, Gels and Colloids*; The Royal Society of Chemistry: Cambridge, UK, 1991; pp 65–80.
- (4) Ananthapadmanabhan, K. P. In *Interactions of Surfactants with Polymers and Proteins*; Goddard, E. D., Ananthapadmanabhan, K. P., Eds.; CRC Press: London, UK, 1993.
- (5) Nnanna, I. A.; Xia, J. D. In *Protein-based Surfactants*; Surfactant Science Series 101; Marcel Dekker: New York, 2001.
- (6) Mesa, C. L. *J. Colloid Interface Sci.* **2005**, *286*, 148–157.
- (7) Kelley, D.; McClements, D. J. *Food Hydrocolloids* **2003**, *17*, 73–85.
- (8) Valstar, A.; Almgren, M.; Brown, W. *Langmuir* **2000**, *16*, 922–927.
- (9) Honda, C.; Kamizono, H.; Matsumoto, K.; Endo, K. *J. Colloid Interface Sci.* **2004**, *278*, 310–317.
- (10) Santos, S. F.; Zanette, D.; Fischer, H.; Itri, R. *J. Colloid Interface Sci.* **2003**, *262*, 400–408.
- (11) Wangsakan, A.; Chinachoti, P.; McClements, D. J. *Langmuir* **2004**, *20*, 3913–3919.
- (12) Few, A. V.; Ottewill, R. H.; Parreira, H. C. *Biochim. Biophys. Acta* **1955**, *18*, 136–137.
- (13) Nozaki, Y.; Reynolds, J. A.; Tanford, C. *J. Biol. Chem.* **1974**, *249*, 4452–4459.
- (14) Turro, N. J.; Lei, X.-G.; Ananthapadmanabhan, K. P.; Aronson, M. *Langmuir* **1995**, *11*, 2525–2533.
- (15) Menger, F. M.; Littau, C. A. *J. Am. Chem. Soc.* **1991**, *113*, 1451–1452.
- (16) Rosen, M. J. *CHEMTECH* **1993**, *23*, 30–33.
- (17) Menger, F. M.; Littau, C. A. *J. Am. Chem. Soc.* **1993**, *115*, 10083–10090.
- (18) Zana, R.; Xia, J. In *Gemini Surfactants*; Zana, R., Xia, J., Eds.; Marcel Dekker: New York, 2004.
- (19) Peters, T. J. In *All about Albumin Biochemistry, Genetics, and Medical Applications*; Peter, T. J., Ed.; Academic Press: San Diego, CA, 1996.
- (20) Foster, J. F. In *Albumin Structure, Function and Uses*; Rosenoer, V. M., Oratz, M., Rothschild, M. A., Eds.; Pergamon Press: Oxford, U.K., 1977; pp 53–84.
- (21) Giancola, C.; De Sena, C.; Fessas, D.; Graziano, G.; Barone, G. *Int. J. Biol. Macromol.* **1997**, *20*, 193–204.
- (22) Magdassi, S.; Vinetsky, Y.; Relkin, P. *Colloids Surf. B* **1996**, *6*, 353–362.
- (23) Sober, H. A.; Harte, R. A. In *Handbook of Biochemistry (Selected Data for Molecular Biology)*; Harte, R. A., Ed.; CRC Press: Cleveland, OH, 1973; p C-71.
- (24) Gucker, F. T., Jr.; Pickard, H. B.; Planck, R. W. *J. Am. Chem. Soc.* **1939**, *61*, 459–470.

- (25) Husband, F. A.; Garrood, M. J.; Mackie, A. R.; Burnett, G. R.; Wilde, P. J. *J. Agric. Food Chem.* **2001**, *49*, 859–866.
- (26) Kreshech, G. C.; Haragraves, W. A. *J. Colloid Interface Sci.* **1974**, *48*, 481–493.
- (27) Andersson, B.; Olofsson, G. *J. Chem. Soc., Faraday Trans. 1* **1988**, *84*, 4087–4095.
- (28) Wang, X. Y.; Li, Y. J.; Li, J. X.; Wang, J. B.; Wang, Y. L.; Guo, Z. X.; Yan, H. K. *J. Phys. Chem. B* **2005**, *109*, 10807–10812.
- (29) Wang, X. Y.; Li, Y. J.; Wang, J. B.; Wang, Y. L.; Ye, J. P.; Yan, H. K.; Zhang, J.; Thomas, R. K. *J. Phys. Chem. B* **2005**, *109*, 12850–12855.
- (30) Zana, R.; Benraou, M.; Rueff, R. *Langmuir* **1991**, *7*, 1072–1075.
- (31) Grosmaire, L.; Chorro, M.; Chorro, C.; Partyka, S.; Zana, R. *J. Colloid Interface Sci.* **2002**, *246*, 175–181.
- (32) Zana, R. *Langmuir* **1996**, *12*, 1208–1211.
- (33) Dubin, P. L.; Vea, M. E. Y.; Fallon, M. A.; Thé, S. S.; Rigsbee, D. R.; Gan, L. M. *Langmuir* **1990**, *6*, 1422–1427.
- (34) Sudbeck, E. A.; Dubin, P. L.; Curran, M. E.; Skelton, J. *J. Colloid Interface Sci.* **1991**, *142*, 512–517.
- (35) Xia, J.; Zhang, H.; Rigsbee, D. R.; Dubin, P. L.; Shaikh, T. *Macromolecules* **1993**, *26*, 2759–2766.
- (36) Carter, D.; Chang, B.; Ho, J. X.; Keeling, K.; Krishnasami, Z. *Eur. J. Biochem.* **1994**, *226*, 1049–1052.
- (37) Brown, J. R.; Shockley, P. In *Lipid–Protein Interactions*; Wiley: New York, 1982.
- (38) Brown, J. R. In *Albumin Structure, Function, and Uses*; Rosenoer, V. M., Oratz, M., Rothschild, M. A., Eds.; Pergamon: Oxford, UK, 1977; pp 156–179.
- (39) Gelamo, E. L.; Tabak, M. *Spectrochim. Acta A* **2000**, *56*, 2255–2271.
- (40) Moriyama, Y.; Kawasaka, Y.; Takeda, K. *J. Colloid Interface Sci.* **2003**, *257*, 41–46.
- (41) Deep, S.; Ahluwalia, J. C. *Phys. Chem. Chem. Phys.* **2001**, *3*, 4583–4591.